A Structural Origin of Latency Relaxation in Frog Skeletal Muscle

Naoto Yagi
SPring-8/JASRI, Kouto, Sayo, Hyogo 679-5198, Japan

ABSTRACT A time-resolved x-ray diffraction study at a time resolution of 0.53 ms was made to investigate the structural origin of latency relaxation (LR) in frog skeletal muscle. Intensity and spacing measurements were made on meridional reflections from the Ca-binding protein troponin and the thick filament and on layer lines from the thin filament. At 16°C, the intensity and spacing of all reflections started to change at 4 ms, simultaneously with the LR. At 0°C, the intensity of the troponin reflection and the layer lines from the thin filament and the spacing of the 14.3-nm myosin meridional reflection, but not the spacing of other myosin meridional reflections, began to change at ~15 ms, when the LR also started. Intensity of myosin-based reflections started to change later. When the muscle was stretched to nonoverlap length, the intensity and spacing changes of the myosin reflections disappeared. The simultaneous spacing change of the 14.3-nm myosin meridional reflection with the LR suggests that detachment of myosin heads that are bound to actin in the resting muscle is the cause of the LR.

INTRODUCTION

A skeletal muscle undergoes a short period of tension decrease after an electrical stimulus. This phenomenon is called latency relaxation (LR) and has been studied for more than 80 years (1–7). The amplitude of the LR increases with sarcomere length up to 2.8–3.0 μm and becomes reduced at longer lengths. Up to 2.8 μm, the time to the maximum amplitude increases with sarcomere length, but the time of onset of the LR does not depend on the length (5,6). An early study showed that the onset of the calcium transient measured by arsenazo III coincided with that of the LR (8). However, recent studies using faster dyes have shown that the calcium transient is much faster (9), and now it seems that the LR takes place considerably after the rise of cytoplasmic calcium concentration.

The origin of the LR is important to understand the elastic properties of resting muscle, which play a significant role in the physiological function of skeletal muscle in vivo (2). Because the LR is a decrease of resting tension, the nature of resting tension in skeletal muscle must be understood to explain it. It is known that there is a short-range elastic component (SREC) in a resting muscle that reacts to an applied stretch in a nonlinear manner (10). The origin of the SREC was considered to be myosin heads that are bound to actin in the resting state, and their detachment was proposed to be the cause of the LR. Similar suggestions have been made by others (1,2). It is now known that the major contributing factor to the passive length-tension relation of striated muscle is a giant extensible protein, titin/connectin, which spans each half-sarcomere and connects the Z-line to the thick filament (11,12). Thus, a structural change in titin may lower the resting tension. Because titin has a calcium-binding region in its PEVK region (13,14), a structural change may be induced by an increase in intracellular calcium concentration.

This x-ray diffraction study is an extension of the previous study (15) to explore the origin of the LR. Two types of experiments were made. In one experiment, the temperature was changed to compare time courses of the structural changes and the LR. In the other experiment, the structural changes at long sarcomere length (3.6 μm), where the overlap between the thick and thin filaments was greatly reduced, were investigated. At all temperatures, the intensity of the troponin reflection and the layer lines from the thin filament and the spacing of the 14.3-nm myosin meridional reflection began to change simultaneously with the LR. The spacing change was not observed with other myosin meridional reflections, suggesting that the origin of the LR is not a structural change in the shaft of the thick filament.

MATERIALS AND METHODS

X-ray diffraction techniques

X-ray diffraction experiments were made using the BL40XU beamline (16) at the SPring-8 third-generation synchrotron radiation facility (Sayo, Hyogo, Japan). The ring current was 100-70 mA, and the specimen-to-detector distance was 2.8 m. The x-ray energy was either 10.5 or 15.0 keV. Combination of Ni and Rh coating of the two focusing mirrors was used. The energy bandwidth was ~2% at 10.5 keV and 3% at 15.0 keV. At 10.5 keV, the flux without attenuation was 8×10^{14} cps. However, it was reduced ~4-fold by an aluminum absorber to avoid radiation damage. Thus, the flux was $\sim 2 \times 10^{14}$ cps. Experiments on the first and second actin layer lines (at around an axial Bragg spacing of 36 and 18 nm, respectively) were made with 15.0-keV x-rays for which the full flux was 6×10^{14} cps. Because these layer lines are at a larger angle in the equatorial direction than other reflections, it was necessary to use shorter-wavelength (higher-energy) x-rays to record them with the detector and camera length used in this experiment. At 15.0 keV, no attenuation was used because the radiation damage was not severe. The size of the beam was adjusted to 0.25 mm horizontally and 0.15 mm vertically (full width at half-maximum) at the specimen. For the measurement on the actin layer lines at 1/5.9 and 1/5.1 nm^{-1}, the camera length was 1.5 m, and the x-ray energy 15.0 keV.

Submitted June 7, 2006, and accepted for publication September 6, 2006.

Address reprint requests to N. Yagi, SPring-8/JASRI, 1-1-1 Kouto, Sayo, Hyogo 679-5198, Japan. Tel.: 81-791-58-0908; Fax: 81-791-58-0830; E-mail: yagi@spring8.or.jp.

© 2007 by the Biophysical Society

0006-3495/07/01/162/10 $2.00

doi: 10.1529/biophysj.106.090696

X-ray diffraction patterns were recorded using an x-ray image intensifier (V5445P, Hamamatsu Photonics, Hamamatsu, Japan) (17) coupled with a fast charge-coupled device (CCD) camera (C7770, Hamamatsu Photonics) (15,18). This camera has three CCD chips that are exposed and read out alternately to achieve a high frame rate. It can record 290 frames per second with a full frame of 640 × 480 pixels in 10 bits. The frame rate can be further increased by reducing the number of vertical pixels. In the current study, each frame had 640 × 72 pixels with a frame rate of 1887 per second (0.53 ms per frame). The camera was rotated by 90° so that the vertical direction of the CCD (with a variable number of pixels) was parallel to the equator of the muscle diffraction pattern and the horizontal direction (with 640 pixels) was parallel to the meridian. To record the first and second actin layer lines, the detector was shifted by ~0.25 nm^{-1} along the equator so that the strongest part of the second layer-line was recorded. Because the gains of the preamplifiers for every CCD were different, a correction (smaller than 6%) was made for the detector response. Even after this correction, a regular three-frame variation of intensity sometimes remained (for example, Fig. 1 *d*).

Muscle preparation

The specimens were sartorius and semitendinosus muscles of a small (body length 6–8 cm) bullfrog (*Rana catesbeiana*). Wild frogs were captured and stored at 9°C for 2–3 days before the experiment. The experiment at 0°C was made in early October, and other experiments were made in winter. The frog was decapitated and quickly pithed, and then a muscle was dissected. The muscle was mounted vertically in a specimen chamber, through which a Ringer's solution containing 115 mM NaCl, 2.5 mM KCl, 1.8 mM $CaCl_2$, 3.0 mM Hepes (pH adjusted to 7.2 at 25°C) was circulated. The temperature was controlled by cooling the Ringer's solution. To avoid radiation damage, the specimen chamber was moved downward at a speed of 100 mm/s during an x-ray exposure (19). The specimen chamber had a pair of silver electrodes, which were placed along the two sides of the muscle to induce field stimulation. The muscle was stimulated with a single supramaximal electric pulse of 0.5 ms duration. Timing of the pulse was adjusted so that its rising edge coincided with beginning of a CCD frame. The sarcomere length was adjusted with laser diffraction. Tension was measured by either one of the following two transducers. One was a semiconductor gauge with high sensitivity (AE801, AME Bioscience, SensNor, Horten, Norway) with a resonant frequency of ~2 kHz, which was used to measure the LR. The other was a strain gauge transducer (UT-100, Minebea, Japan, with a resonant frequency of 300 Hz), which was mainly used to measure the peak twitch tension. Tension signal was recorded digitally at a sampling rate of 20 kHz. Because a small tension change was difficult to measure when the specimen was moving, the LR was measured separately without moving the specimen chamber. Even in this case, the LR in each tension trace was not easy to measure because of the vibration and electrical noises in the environment. Thus, the LR was estimated after traces of contractions from several muscles were added. Because the LR tends to become smaller with repeated twitches, it was measured before the x-ray experiment.

The x-ray data collection on each muscle was repeated 10–15 times. No significant deterioration of twitch tension was noticed. After each data recording, the specimen was moved sideways by 0.5 mm, so that the same part of the muscle was not irradiated by x-rays twice. No sign of radiation damage was observed under a light microscope after an experiment.

Data processing

The procedures for data processing were essentially the same as in the previous study, for which representative intensity profiles were shown (15).

Each x-ray meridional diffraction pattern was rotated by using the two diffraction spots of the third-order myosin meridional reflection on either side of the equator as a guide for the axes. Images of the same frame number were summed over experiments on each muscle. Quadrant averaging was also done. A meridional intensity profile was obtained by integrating the intensity in the lateral region of 0 to 0.0051 nm^{-1}. Then, for the second to sixth myosin meridional reflections, background was subtracted by linearly connecting the regions on the two sides of the reflection. The area above the background was taken as the integrated intensity. The intensity was normalized by that before a stimulus, and the results were averaged over different muscles. The x-rays used in this experiment had an energy bandwidth of ~3% and an asymmetric energy profile that had a longer tail toward lower energies (16). Thus, a peak profile of a meridional reflection had a tail toward wider angles. This made it inappropriate to use the center of gravity of an intensity peak for its position. Therefore, the position was obtained by calculating the center of gravity of only five data points around the peak (the peak point and two points on each side of the peak point) after a linear background subtraction. Because each meridional reflection consisted of more than one peak (20) that could not be resolved in this experiment, this gives an average spacing of a cluster of peaks. Although the positions of the three CCD chips were adjusted by the manufacturer to one-third of the pixel size, the spacing changes measured in this study were much smaller than the pixel size on the CCD chips. Thus, it was necessary to correct for the misalignment of the three CCD chips. Even after this was done, the data points sometimes showed a tendency to cluster in three points (for example, Fig. 1 *b*). The Bragg spacings of the third- and the sixth-order myosin meridional reflections were assumed to be 14.3 and 7.2 nm, respectively, in the resting state. For the data that do not require high time resolution (those obtained at 0°C), three frames were summed before the data processing so that the differences in gain and position of the three CCD chips did not affect the results.

To measure the intensity of the meridional reflections from C-protein and troponin, at ~1/44.1 and 1/38.5 nm^{-1}, respectively, a fitting procedure was used (15). The intensity profile was fitted with a sum of three peaks and a fourth-order polynomial background using a modified Levenberg-Marquardt algorithm (subroutine UNLSF in the IMSL library, Visual Numerics, San Ramon, CA). The highest points of the peaks were fixed at 1/46, 1/44.1, and 1/38.5 nm^{-1}. The first small peak at 1/46 nm^{-1} actually consists of two or more meridional reflections of an unknown origin (20). The troponin and C-protein reflections are also split into two peaks, but these cannot be resolved in this study. For the profile fitting, the intensity profile of the meridional reflection at 1/14.3 nm^{-1} was obtained after linear background subtraction. Then it was converted to the energy profile by normalization by the distance between the peak position and the direct beam. When normalized by the distance from the origin of the diffraction pattern, the profiles of the 46-, 44.1-, and 38.5-nm reflections are expected to be broader than that of the 14.3-nm reflection because of the vertical beam size (~0.2 mm at the detector) and the spatial resolution of the x-ray detector (~0.3 mm). The observed profile is a convolution of the intrinsic width of the reflection with the energy spread, the beam size, and the spatial resolution. To simulate this, the profile obtained from the 14.3-nm reflection was broadened to fit the peaks of the three reflections. Broadening of 200% gave the most satisfactory result. The fit was generally good enough to separate contributions from the three reflections (15).

The lateral width of a meridional reflection was obtained in a one-pixel axial section (parallel to the equator) that passes through the peak of the reflection. The axial width of the section (one pixel) corresponds to a meridional spacing of 0.00065 nm^{-1}. The background was removed by linearly extrapolating the intensity distribution in the region of 0.005–0.010 nm^{-1} toward the meridian. The full width at half-maximum was obtained by interpolation between data points. The beam size and the spatial resolution of the detector (see above) accounted for 1–2 pixels (~0.001 nm^{-1}) of the width.

The intensities of the first and second actin layer lines (at 1/36 and 1/18 nm^{-1} axially, respectively) were measured by fitting a fourth-order polynomial background plus two Gaussian peaks. For the second-order layer line, whose intensity was very low in the resting state and increased after a stimulus, the intensity was normalized between zero and a peak value.

For the measurement on the actin layer lines at 1/5.9 and 1/5.1 nm^{-1}, a very simple method was used to estimate the integrated intensity and the

axial spacing. Background regions were identified from the first to the sixth myosin and 5.9- and 5.1-nm actin layer lines, and a line was drawn between them. The area above the background was taken as the integrated intensity, and the center of gravity of the intensity above background was taken as the position of the layer line. This method has an obvious fault in that it overestimates the background, which is generally convex downward. Also, it does not give an exact peak position because of the axially asymmetric profile of the layer lines, which is caused by the asymmetric energy profile. Another serious problem with the actin layer lines is that, because of the low energy resolution, the seventh and eighth myosin layer lines are not separated from the actin layer lines. Thus, the intensity of the seventh myosin layer line is included in that of the 5.9-nm actin layer line. On the other hand, because the eighth layer line is between the 5.9-nm and 5.1-nm actin layer lines, it is treated as background. The intensity changes of these myosin layer lines affect the apparent integrated intensity and peak position of the actin layer lines. However, in the early stage of contraction, the intensity change of the myosin layer lines is slower than that of the actin layer lines, making it possible to study the early changes in the actin layer lines.

Simulation

For simulation, a meridional intensity profile was calculated on an array of points separated by 14.3 nm, which simulates myosin heads along the thick filament. There are 49 points of myosin heads on each half of the thick filament with the third row from the tip missing (21). The first point is at 86.5 nm from the center of the filament. This gives a peak of the 14.3-nm reflection with a small subsidiary peak on the higher-angle side, as experimentally observed (22). The myosin heads were assumed to be regularly spaced at 14.3-nm intervals. An axial intensity profile was calculated by Fourier transform of the two symmetric arrays of the myosin heads in the thick filament and convoluted with the actual profile of the 14.3-nm meridional reflection to take the energy spread and the beam size into account. The resultant intensity profile was sampled at 0.00065 nm^{-1} to simulate the actual detector resolution, and five data pixels across the peak of the 14.3-nm reflection were used to estimate its axial spacing. For the effects of detachment of myosin heads from actin, it was assumed that randomly chosen 10–40% of the heads in the overlap region at a sarcomere length of 2.6 μm, which represented bound heads, were shifted from their regular positions in the resting state by 3.6 nm toward the tip and that after detachment they were axially disordered and did not contribute to the meridional intensity. The calculation was repeated 1000 times with different random numbers, and the intensity distribution was averaged.

RESULTS

Sartorius muscle at 16°C and 2.6 μm

In the previous study (15), changes in the x-ray diffraction intensity and Bragg spacing of the meridional reflections were measured at 8°C and 12°C. However, because the Ca^{2+} transients are usually measured at 16°C (9), the measurement on the meridional reflections was repeated at 16°C (Fig. 1). The sarcomere length was adjusted to 2.6 μm so that the LR was measured clearly.

At the time resolution of 0.53 ms, the intensity of the meridional reflections from myosin (at 1/21.5, 1/14.3, and 1/7.2 nm^{-1}, Fig. 1, *a* and *c*), from troponin (at 1/38.5 nm^{-1}, Fig. 1 *d*), and from C-protein (1/44.1 nm^{-1}, Fig. 1 *c*) all started to change at ~4 ms after the onset of a stimulus. The Bragg spacing of the 14.3-nm meridional reflection began to decrease at 4 ms and reached a minimum at 7 ms, whereas that of the 7.2-nm reflection began to increase at ~5 ms without a decrease (Fig. 1 *b*). The maximum reduction in the 14.3-nm spacing was 0.046%. The reduction in the Bragg spacing was not observed in the 21.5-nm meridional reflection. The intensity of the 38.5-nm troponin reflection reached a maximum increase of 27% at 9 ms and then declined to 50% at 35 ms (Fig. 1 *d*). Lateral width of this reflection across the meridian was 0.0024 nm^{-1} in the resting state and started to increase at ~4 ms and was 0.0043 nm^{-1} at 35 ms. Thus, if the net integrated intensity is assumed to be the apparent integrated intensity multiplied by its lateral width (23), the net intensity at 35 ms was ~90% of that before the stimulus. All these changes were similar to those observed at lower temperatures (15) but faster. The LR also began at ~4 ms, and the tension began to increase at 4.8 ms (Fig. 1 *e*). Its maximum amplitude was 0.37 mN (an average of 12 contractions in 12 muscles). Twitch tension was 0.72 ± 0.03 N (mean ± SE, $n = 9$), and the time to peak tension was 35.8 ± 0.8 ms ($n = 9$).

At this temperature, most structural changes began simultaneously at 0.53 ms time resolution. Thus, it was difficult to discriminate the time courses of the structural changes in troponin and myosin. However, the calcium binding of troponin calculated using fluorescence from Ca^{2+} indicators is almost saturated at 4 ms (9). Even considering the difference in the species of frogs and the seasonal effect, it can be concluded that the intensity and spacing changes do not take place in parallel with the increase in the intracellular calcium concentration or calcium binding by troponin but are delayed considerably. This also demonstrates that the LR is not associated with the excitation-contraction coupling or a process of calcium release, as previously proposed (24).

Sartorius muscle at 0°C and 2.6 μm

To clarify the temporal relations among the intensity and spacing changes and the LR, an experiment at a low temperature was performed. This experiment was made in early October when the frogs were still adapted to the climate in summer, and thus, contraction at low temperature was very slow. The intensity of the myosin reflections at 1/14.3 and 1/21.5 nm^{-1} began to change at ~20 ms after the stimulus (Fig. 2 *a*). The intensity of the 14.3-nm reflection increased slightly before it decreased. The intensity of the 44.1-nm C-protein reflection also started to decrease slowly, at ~25 ms (Fig. 2 *a*). On the other hand, the intensity of the 38.5-nm troponin reflection (Fig. 2 *a*) and the spacing of the 14.3-nm myosin reflection (Fig. 2 *b*) started to change at ~10–15 ms. The intensity of the 38.5-nm reflection reached 32% above its resting level at 32 ms and then decreased. The maximum spacing decrease of the 14.3-nm reflection was 0.014%, which was smaller than that observed at 16°C (0.046%, see above). The intensity of the layer lines from the thin filament at 1/36 and 1/18 nm^{-1} also started to change at ~15 ms (Fig.

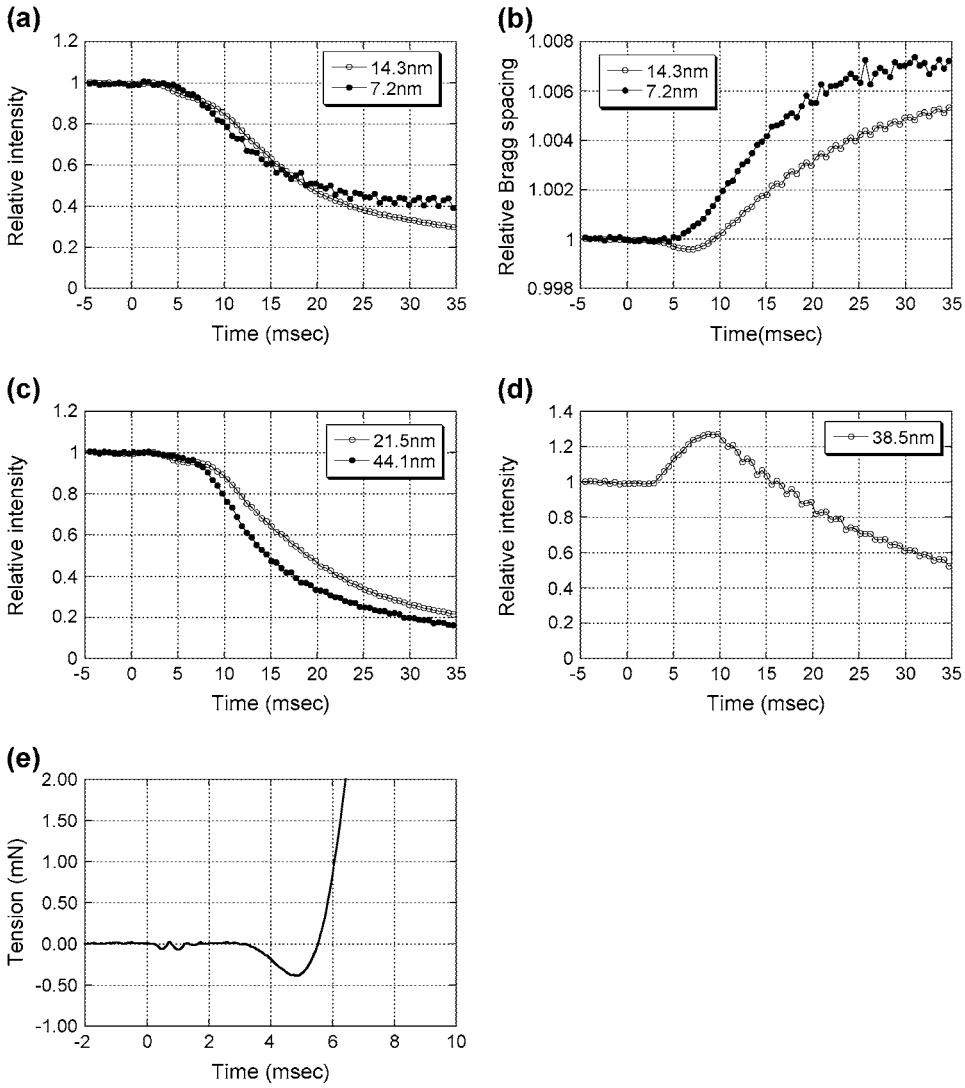

FIGURE 1 Intensity, spacing, and tension recorded in an early stage of twitch of frog sartorius muscle at 16°C. Time resolution of the x-ray recording was 0.53 ms. (*a*) Intensity changes of the myosin meridional reflections at 1/14.3 (*open circles*) and 1/7.2 (*solid circles*) nm^{-1}. The approximate intensity before the stimulation was 73,000 photons per 0.53 ms for the 14.3-nm reflection and 2000 photons for the 7.2-nm reflection. (*b*) Changes in the Bragg spacing of the meridional reflections at 1/14.3 (*open circles*) and 1/7.2 (*solid circles*) nm^{-1}. (*c*) Intensity changes of the myosin meridional reflections at 1/21.5 (*open circles*) and 1/44.1 (*solid circles*) nm^{-1}. The average intensity before the stimulation was 32,000 photons for the 21.5-nm reflection and 61,000 photons for the 44.1-nm reflection. (*d*) Intensity change of the troponin meridional reflection at 1/38.5 nm^{-1}. The intensity before the stimulation was 18,000 photons. (*e*) Tension, which is an average of 12 twitches of 12 muscles. (*a–d*) Based on data from 148 twitches of 19 muscles.

2 *c*). The LR began at ~15 ms and reached a minimum, which was 0.62 mN below the resting tension (an average of 43 traces in 4 muscles), at ~18 ms (Fig. 2 *d*). The peak twitch tension was not measured. These results show that the Ca^{2+}-induced structural changes in both the thick and thin filaments take place earlier (at 10–15 ms) than the actin-myosin interaction (at 20 ms). The LR seems to be related to the former.

Semitendinosus muscle at 16°C, at 2.6 and 3.6 μm

To find the effects of filament overlap on the meridional intensity and spacing changes, the measurements on the meridional reflections were made on semitendinosus muscle, which can easily be stretched to a sarcomere length at which there was no overlap between the thick and thin filaments. The temperature was 16°C. The results of control experiments at 2.6 μm (Fig. 3, *solid circles*) were essentially the same as those on sartorius muscle (Fig. 1). The intensity of all reflections started to change at ~4 ms after the onset of the stimulus. The 7.2-nm and 21.5-nm reflections began to change slightly later (starting to change at 5 ms, Fig. 3, *c* and *e*) and the 38.5-nm meridional reflection slightly earlier (starting at 3 ms, Fig. 3 *f*). The maximum increase in the 38.5-nm reflection intensity was 24% (Fig. 3 *g*). Lateral width of this reflection across the meridian was 0.0029 nm^{-1} in the resting state, started to increase at ~4 ms, and was 0.0034 nm^{-1} at 35 ms. The reason for the smaller increase than in sartorius muscle (0.0024 to 0.0043 nm^{-1} on contraction, see above) is unknown. However, the intensity of the troponin reflection did not decrease as much as in sartorius muscle (Fig. 1 *d*), probably because of the smaller increase in the lateral width. The Bragg spacing of the 14.3-nm reflection began to decrease at ~4 ms and reached a minimum of 0.04% decrease at ~7 ms (Fig. 3 *b*), but that of the 7.2-nm or 21.5-nm reflection did not decrease (Fig. 3, *d* and *f*). The LR began at 3.5 ms and the tension reached a maximum drop of 1.2 mN (an average of nine contractions

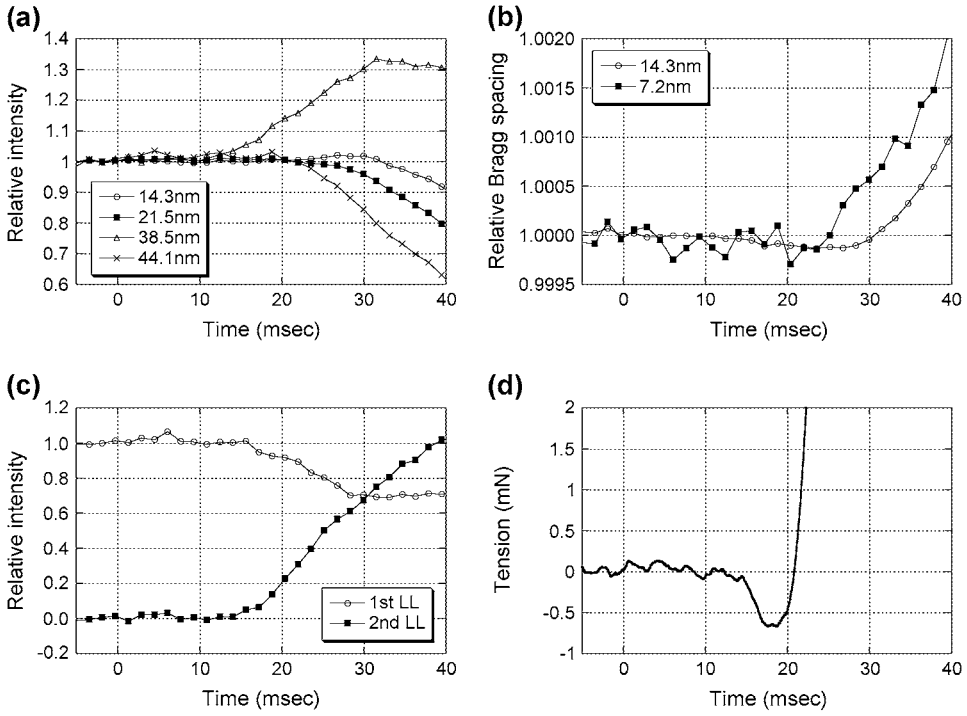

FIGURE 2 Intensity, spacing, and tension recorded in an early stage of twitch of frog sartorius muscle at 0°C. Time resolution of the x-ray recording was 1.6 ms. (*a*) Intensity changes of the meridional reflections at 1/14.3 (*open circles*), 1/21.5 (*solid squares*), 1/38.5 (*open triangles*), and 1/44.1 (*crosses*) nm^{-1}. The intensity before the stimulation was 27,000 photons per 1.6 ms for the 14.3-nm reflection, 20,000 photons for the 21.5-nm reflection, 24,000 for the 38.5-nm reflection, and 23,000 photons for the 44.1-nm reflection. (*b*) Changes in the Bragg spacing of the myosin meridional reflections at 1/14.3 (*open circles*) and 1/7.2 (*solid squares*) nm^{-1}. (*c*) Intensity changes of the actin layer lines at 1/36 (*open circles*) and 1/18 (*solid squares*) nm^{-1}. The intensity before the stimulation was 36,000 photons for the 36-nm layer line, and the intensity at 40 ms was 31,000 photons for the 18-nm layer line. (*d*) Tension, which is an average of five twitches of five muscles. (*a* and *b*) Based on data from 88 twitches of eight muscles. (*c*) Based on data from 108 twitches of 16 muscles.

in nine muscles) at 5.2 ms (Fig. 3 *h*). Peak twitch tension was 0.33 ± 0.02 N ($n = 9$) and the time to peak tension was 48.7 ± 1.0 ms ($n = 9$).

At a sarcomere length of 3.6 μm, there is little overlap between the thick and thin filaments. Peak twitch tension was 0.05 ± 0.01 N ($n = 8$), and the time to peak tension was 49.6 ± 1.5 ms ($n = 8$). This tension is supposed to be caused by contraction of sarcomeres near the ends of muscle fibers that are not stretched to the nonoverlap length (25). The LR was difficult to measure because of the high resting tension (0.24 ± 0.04 N, $n = 8$), but previous studies on single isolated fibers showed that the LR is reduced at this sarcomere length (6).

Stretch caused reduction in the intensity of myosin reflections in the resting state (26). The intensity changes of the myosin reflections during stimulation also became smaller (27), the 14.3-nm, 7.2-nm, and 21.5-nm reflections showing almost no change (Fig. 3, *a, c*, and *e*, *open circles*). On the other hand, the intensity increase of the 38.5-nm troponin was larger at 3.6 μm, with a peak intensification by 110% (Fig. 3 *g*). The lateral width of this reflection was 0.0045 nm^{-1} in the resting state and did not change on stimulation. This suggests that actin-myosin interaction suppresses the intensity of the 38.5-nm reflection during contraction at a shorter sarcomere length. The stretch caused an increase of 0.25% in the Bragg spacing of the 14.3-nm meridional reflection (Fig. 3 *b*), 0.31% in the 7.2-nm meridional reflection (Fig. 3 *d*), and 0.44% in the 21.5-nm meridional reflection (Fig. 3 *f*) in the resting state. The early spacing decrease of the 14.3-nm reflection was abolished, but the spacing increased during contraction in all meridional reflections (Fig. 3, *b, d*, and *f*), including the fourth order at 1/10.8 nm^{-1} (data not shown) by ~0.05%. The sizes of the spacing change by stretch (0.3% with resting tension of 0.24 N) and by stimulation (0.05% with twitch tension of 0.05 N) can be explained by extension of the thick filament as a result of the tension on it. The slow rise after stimulation at 3.6 μm may be caused by the tension developed at the ends of fibers (27), which extends the thick filaments through titin, which connects them to the Z-line. Small differences among the spacing changes of the meridional reflections may be caused by different samplings by the interference function. On the other hand, the spacing increase at 2.6 μm during contraction was disproportionately large (1.2% with twitch tension of 0.33 N), suggesting a gross structural change in the thick filament (28).

Changes in the actin layer lines at 1/5.9 and 1/5.1 nm^{-1}

To find possible structural changes in actin that may affect its interaction with myosin, we measured changes in the intensity and spacing of the actin layer lines at 1/5.9 and 1/5.1 nm^{-1}. From the helical structure of the thin filament, tropomyosin and troponin are unlikely to contribute directly to these layer lines. The experiment was made at 6°C. Large frogs were used to ensure high intensity of the diffraction pattern. Because the seventh myosin layer line overlaps with the 5.9-nm actin layer line, and the eighth myosin layer line is located between the two actin layer lines but not resolved from them, intensity changes of myosin layer lines were first studied to find the time courses of their intensity changes.

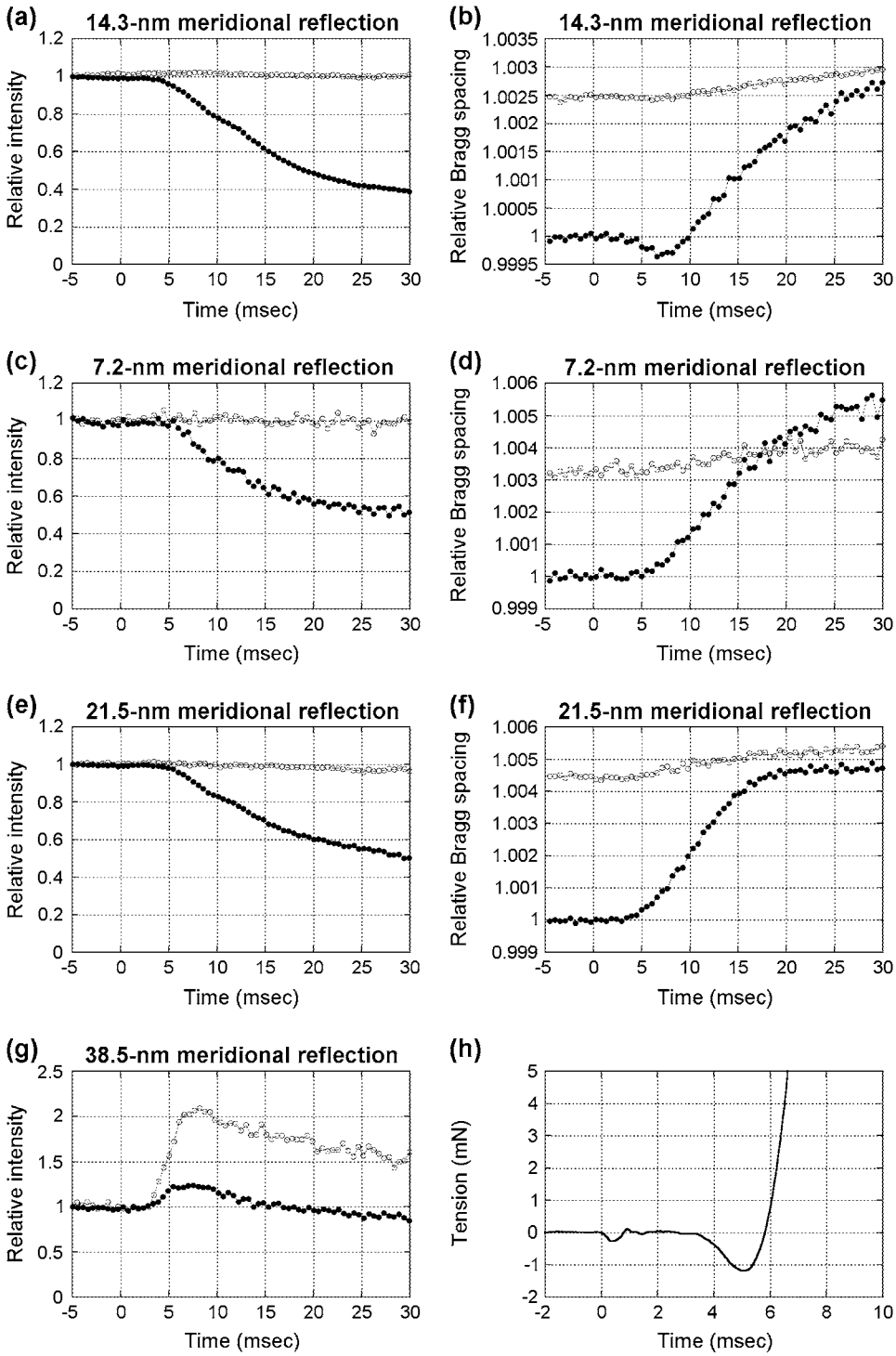

FIGURE 3 Intensity, spacing, and tension recorded in an early stage of twitch of frog semitendinosus muscle at 2.6 μm (*black*) and 3.6 μm (*shaded*) at 16°C. Time resolution of the x-ray recording was 0.53 ms. (*a*) Intensity changes of the myosin meridional reflection at 1/14.3 nm^{-1}. The intensity before the stimulation was 86,000 photons per 0.53 ms at 2.6 μm and 16,000 photons at 3.6 μm. (*b*) Changes in the Bragg spacing of the myosin meridional reflection at 1/14.3 nm^{-1}. (*c*) Intensity changes of the myosin meridional reflection at 1/7.2 nm^{-1}. The intensity before the stimulation was 2200 photons at 2.6 μm and 590 photons at 3.6 μm. (*d*) Changes in the Bragg spacing of the myosin meridional reflection at 1/7.2 nm^{-1}. (*e*) Intensity changes of the myosin meridional reflection at 1/21.5 nm^{-1}. The intensity before the stimulation was 40,000 photons at 2.6 μm and 6000 photons at 3.6 μm. (*f*) Changes in the Bragg spacing of the myosin meridional reflection at 1/21.5 nm^{-1}. Because there are several peaks in the region of this reflection, the Bragg spacing shown here is a weighted average of these peaks. (*g*) Intensity changes of the troponin meridional reflection at 1/38.5 nm^{-1}. The intensity before the stimulation was 14,000 photons at 2.6 μm and 3400 photons at 3.6 μm. (*h*) Tension, which is an average of 16 twitches of 16 muscles. The results at 2.6 μm are based on data from 97 twitches of 14 muscles. The results at 3.6 μm are based on data from 111 twitches of 22 muscles.

Fig. 4 *a* shows the intensity change of the first myosin layer line at ~1/43 nm^{-1} in sartorius muscle. The intensity of its inner region began to decrease at ~12 ms after an electrical stimulus. On the other hand, the intensity of its outer region, where it overlaps with the first actin layer line at ~1/36 nm^{-1}, started to decrease at ~7 ms after a stimulus. Thus, it is likely that the intensity change between 7 and 12 ms after a stimulus is mostly that of the first actin layer line. This is confirmed by the spacing measurement shown in Fig. 4 *b*. As the intensity of the actin layer line began to decrease at ~7 ms, the apparent spacing of the outer part of the layer line increased because there was less contribution from the actin layer line, which is located on the high angle side (that is smaller Bragg spacing) of the layer line. When the

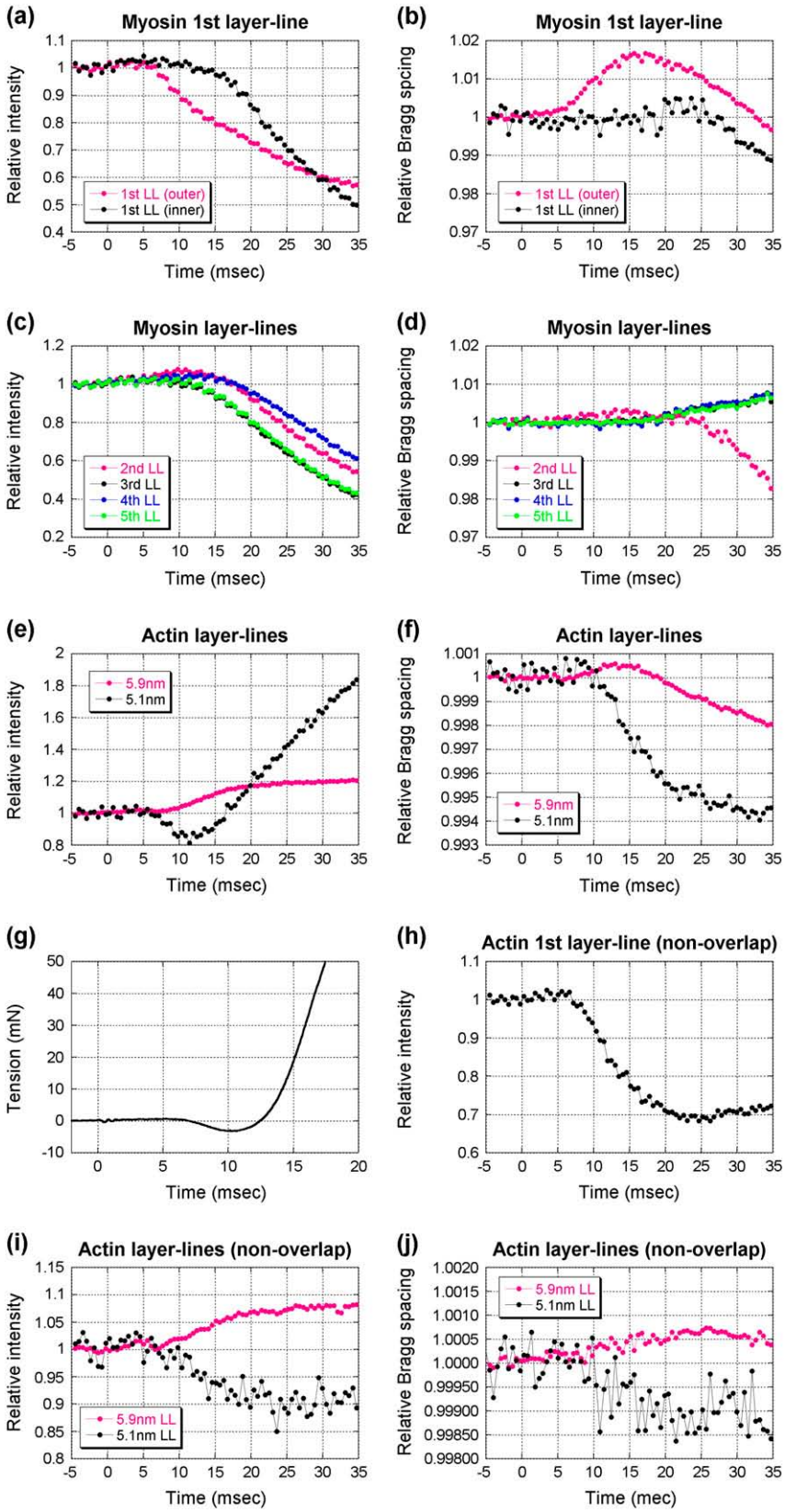

FIGURE 4 Intensity, spacing, and tension recorded in an early stage of twitch of frog sartorius muscle (*a–g*) and semitendinosus muscle (*h–j*) at 6°C. An electrical stimulus was given at time zero. All data are normalized with the average intensity observed within 5 ms before the stimulus. (*a*) Intensity changes of the inner (*black*) and outer (*red*) regions of the first myosin layer line at ~1/43 nm^{-1}. For the outer region, the area of lateral integration was 0.078–0.113 nm^{-1}, and the average intensity before the stimulus was 55,000 photons. For the inner region, the area of lateral integration was 0.042–0.078 nm^{-1}, and the average intensity before the stimulus was 220,000 photons. (*b*) Spacing changes of the inner (*black*) and outer (*red*) regions of the first myosin layer line. (*c*) Intensity changes of the second (*red*), third (*black*), fourth (*blue*), and fifth (*green*) myosin layer lines. The data for the third and fifth layer lines mostly overlap. The area of lateral integration was 0.060–0.113 nm^{-1} for the second layer line and 0.042–0.078 nm^{-1} for the others. The average intensities before the stimulus were 47,000, 55,000, 40,000, and 29,000 photons for the second-, third-, fourth-, and fifth-order layer lines, respectively. (*d*) Spacing changes of the second (*red*), third (*black*), fourth (*blue*), and fifth (*green*) myosin layer lines. The data for the third, fourth, and fifth layer lines mostly overlap. (*e*) Intensity changes of the actin layer lines at 1/5.9 (*red*) and 1/5.1 (*black*) nm^{-1}. The areas of lateral integration were 0.042–0.112 and 0.042–0.087 nm^{-1} for the 5.9- and 5.1-nm layer lines, respectively. The average intensities before the stimulus were 158,000 and 8000 photons for the 5.9- and 5.1-nm layer lines, respectively. (*f*) Spacing changes of the actin layer lines at 1/5.9 (*red*) and 1/5.1 (*black*) nm^{-1}. (*g*) Representative tension response of sartorius muscle after a single electrical stimulus at time zero. (*h*) Intensity change of the first actin layer line in an overstretched semitendinosus muscle. The area of lateral integration was 0.078–0.112 nm^{-1}. The average intensity before the stimulus was 40,000 photons. Because the first actin and the first myosin layer lines overlap, the integrated intensity includes that of the first myosin layer line. (*i*) Intensity changes of the actin layer lines at 1/5.9 (*red*) and 1/5.1 (*black*) nm^{-1}. The areas of lateral integration were 0.042–0.112 and 0.042–0.087 nm^{-1} for the 5.9- and 5.1-nm layer lines, respectively. The average intensities before the stimulus were 122,000 and 8000 photons for the 5.9- and 5.1-nm layer lines, respectively. (*j*) Spacing changes of the actin layer lines at 1/5.9 (*red*) and 1/5.1 (*black*) nm^{-1}. The data from sartorius muscles were obtained in a total of 357 twitches of 23 muscles (each muscle contracted 5–19 times), and those from semitendinosus muscles in 184 twitches of 20 muscles (each muscle contracted 5–13 times).

intensity of the 43-nm myosin layer line became low at 25 ms, the Bragg spacing of the both regions of the layer line decreased.

Fig. 4 *c* shows intensity changes of other myosin layer lines. The intensity of the third- and fifth-order layer lines began to decrease at ~12 ms, like the inner part of the first layer line. The intensity of the second layer line (at 1/21.5 nm^{-1}) began to increase at ~7 ms, suggesting an influence of a reflection from the thin filament. One possibility is the second actin layer line at ~1/18 nm^{-1}, which increases in intensity as the first actin layer line weakens (Fig. 2 *c*). Part of intensity of this layer line may have been included in that of the second myosin layer line. The fourth-order myosin layer line at 1/10.8 nm^{-1} also began to increase slightly at ~7 ms. The fourth-order meridional reflection of troponin at 1/9.6 nm^{-1} may have contributed to the intensity of this layer line. The spacing of the myosin layer lines other than the second changed in a very similar manner (Fig. 4 *d*): they started to increase at ~15 ms. This is consistent with the increase in the axial periodicity of the thick filament, which has been observed for many years (20). On the other hand, the spacing of the second layer line decreased, possibly because contribution from the second actin layer line became significant when the intensity of the myosin layer line decreased.

The spacing of the 5.9-nm actin layer line started to increase at ~8 ms (Fig. 4 *e*). The intensity of this layer line was found to increase slightly when an overstretched muscle was stimulated (29). The initial increase before 12 ms may result from the same structural change, although part of the later increase was probably caused by myosin binding to actin. The intensity of the 5.1-nm actin layer line started to decrease at ~7 ms and then began to increase at ~12 ms. The initial decrease seems to be caused by a structural change in actin. The spacing of the 5.9-nm layer line initially increased (Fig. 4 *f*). The spacing decreased in the later phase probably because the seventh myosin layer line (at 1/6.1 nm^{-1}), which is located on the low-angle side of the 5.9-nm actin layer line, became weaker. The spacing of the 5.1-nm actin layer line did not show an initial change but decreased only after 12 ms. Thus, Ca-binding to troponin does not seem to affect the apparent spacing of the thin filament. It should be noticed that the spacing changes shown in Fig. 4 *f*, especially after 12 ms, do not represent the true position of these layer lines. The apparent axial spacings measured in the present study were affected by intensity changes of the myosin layer lines. It is well known that actin spacings increase during contraction (30,31), but they are not measured accurately here.

The LR in this experiment at 6°C started at ~7 ms after a stimulus, and the tension started to increase at ~10 ms (Fig. 4 *g*). Thus, the initial changes in the intensity and spacing that were described above coincided with the beginning of the LR.

Experiments were also made on overstretched semitendinosus muscles, which were dissected from the same frog that was used for the experiments on sartorius muscles described above. The temperature was also the same (6°C). As shown above, the outer region of the first myosin layer line (at 1/43 nm^{-1}) included contribution from the first actin layer line (at 1/36 nm^{-1}). This is confirmed in Fig. 4 *h*, which shows that the intensity of the myosin/actin layer line started to decrease at ~7 ms and continued to decrease afterward. The intensity change observed here probably mostly represents that of the actin layer line because the myosin layer lines are weak in an overstretched muscle (26), and their intensity change on activation is small (27).

The intensity of the 5.9-nm layer line started to increase at ~7 ms and increased by 8% in 25 ms (Fig. 4 *i*). This is consistent with the increase observed by Yagi and Matsubara (29). The intensity of the 5.1-nm layer line started to decrease at ~8 ms and decreased by 10% in 25 ms. Poor statistical power of the data made it difficult to decide when the spacing of the 5.9- and 5.1-nm layer lines started to change (Fig. 4 *j*). Wakabayashi et al. (31) observed in an overstretched muscle that stimulation decreased the Bragg spacing of the 5.9-nm layer line by 0.04% and that of the 5.1-nm layer line by 0.22%. The decrease of 0.1% in the 5.1-nm layer line found in this study may correspond to their result. On the other hand, in the 5.9-nm layer line the result obtained here is an increase, which is opposite to their finding. However, the change is very small in both results.

DISCUSSION

As found in the previous study (15) and confirmed in the study presented here, at the beginning of skeletal muscle contraction, a few events take place almost simultaneously after a considerable fraction of troponin molecules have bound Ca^{2+}:

1. The thin filament, including troponin and tropomyosin, begins to change its structure.
2. The thick filament (either backbone or myosin heads) begins to change its structure, shifting the 14.3-nm meridional reflection toward higher angles. Although a myosin light chain binds Ca^{2+}, its kinetics is known to be too slow to account for this observation (32). Binding of Ca^{2+} to another site must trigger this structural change.
3. A small drop in resting tension (the LR) begins. The present and previous (15) data demonstrate that these events take place simultaneously at different temperatures (0, 8, 12, and 16°C), suggesting strong links among them. These are separate from the interaction of myosin heads with actin, which shows up in the intensity of the myosin and C-protein meridional reflections later (Fig. 2 *a*).

The compliance of the thick filament is considered to be in the order of 0.1% at full tetanic tension (33). Because the size of the LR is 0.05–0.4% of peak twitch tension (3,10), shortening of the thick filament by the LR is only in the order of 0.00005–0.0004%, which is much smaller than the

14.3-nm spacing change observed in this study (0.01–0.04%). Thus, the spacing change is not simply a result of shortening of the thick filament caused by a drop in the resting tension. The most intriguing feature of the spacing change is that only the 14.3-nm reflection shows a temporary decrease. This is unexpected if the spacing change is caused by a change in the axial periodicity or interference between diffraction from the two symmetric cross-bridge regions in the thick filament. When the axial periodicity of myosin molecules does increase during contraction, the spacings of all meridional reflections increase in a similar manner (Fig. 3, *b, d*, and *f*). Thus, the molecular event that coincides with the LR affects the 14.3-nm reflection specifically. This is very hard to explain by a structural change of myosin heads in the thick filament because they are forming a helix. If they undergo a conformational change, the entire diffraction arising from the helix must change.

Detachment of myosin heads that are bound to actin in the resting state has been proposed as the cause of the LR (2,10). This may explain the specific decrease in the spacing of the 14.3-nm reflection and is consistent with the present observation that the early spacing change is abolished at nonoverlap sarcomere length. It is known that in an isometric contraction the reflection, which is at 1/14.5 nm^{-1}, is mostly contributed by heads attached to actin, which is demonstrated by a large-intensity drop after a quick release of muscle (34). Because the myosin heads originate from the thick filament with a regular axial repeat of 14.5 nm, they bind to the thin filament maintaining this spacing on average, giving rise to the meridional reflection (35). The helical arrangement and the axial perturbation of the heads that exists in the relaxed muscle do not influence the pattern of myosin binding to the thin filament during contraction (36). The attached heads are also known to contribute to a relatively smaller extent to the 7.2-nm meridional reflection (34). A small change in conformation of myosin heads may alter the distance between the centers of the two arrays of myosin heads in two symmetric halves of the thick filament, which affects the axial sampling of the 14.3-nm reflection. If detachment causes a conformational change of the heads, the interference distance may change, affecting the apparent spacing. A simple model calculation (see Methods) shows that, if 10% of heads are attached in a conformation with the center of mass shifted toward the Z-line by 3.6 nm, their detachment causes a 0.012% decrease in the apparent Bragg spacing and an intensity decrease of 1.5%. For the 7.2-nm reflection, this model predicts a 0.001% decrease in the apparent spacing and 9% intensity increase. When the heads are assumed to return to the regular 14.3-nm repeat immediately after detachment, the intensity of the 14.3-nm reflection was predicted to increase by 14%, which seems to be too large. The spacing change observed in the experiments was up to 0.046% at 16°C (Fig. 1 *b*). Introducing perturbation in the axial arrangement of myosin heads (22,37) would reduce the calculated intensity of the 14.3-nm reflection and enhance the spacing decrease resulting from detachment, but such a calculation would require a more detailed model of the thick filament structure.

The precise mechanism of the detachment is not clear, but the changes in the structure of the thin filament on binding of calcium to troponin may affect the attached heads. Fig. 4, *e* and *f* show that the intensity and spacing of the actin layer lines at 1/5.9 and 1/5.1 nm^{-1} start to change when the LR begins. Because these layer lines have little contribution from tropomyosin and troponin, the results indicate that Ca^{2+} binding to troponin causes a structural change in actin molecules. Although changes in the parameters of the actin helix are not precisely determined in the present study (Fig. 4, *f* and *j*), it is likely that binding of myosin heads to actin in the resting state is affected when the helical structure changes with calcium (31).

The onset of the LR is known to be unaffected by a stretch of sarcomere (6) even though the distance between the A-band and the Z-line, which is a calcium release site, increases with the stretch. This observation might make cross-bridges an unlikely origin of the LR. However, because the structural change in the thin filament takes place well after calcium ions diffuse through cytoplasm, the diffusion time does not seem to limit the onset of the LR. It is also known that the size of the LR increases with a stretch up to a sarcomere length of 2.8–3.0 μm (6). Because the overlap region between the thick and thin filaments decreases with stretch, this might seem inconsistent with the cross-bridge origin of the LR. However, because the distance between the thick and thin filaments decreases with a stretch, the number of attached heads in the resting state may increase.

Another possible origin of the LR is a calcium-induced structural change of titin. However, it is unclear how a conformational change of titin can cause an apparent shift of the peak position of only the 14.3-nm myosin meridional reflection. If the myosin periodicity in the thick filament changes, positions of all meridional reflections should be affected. As examined above, the apparent spacing change is much larger than that expected from the change in tension by the LR. Thus, the spacing change cannot be explained by a simple decrease of tension on the thick filament. Although it is still possible that the stiffness change in titin is the cause of the LR and the spacing change of the 14.3-nm meridional reflection has another cause, the close correlation between the LR and the spacing change at different temperatures makes this possibility unlikely.

In conclusion, our data show that the LR is not caused by a process in the excitation-contraction coupling or calcium release. Structural changes in both the thick and thin filaments and the tension drop of the LR begin simultaneously, suggesting that the LR involves detachment of cross-bridges from the thin filament.

I thank Dr. H. Iwamoto for the use of the specimen stage, Dr. K. Inoue for the beam-line operation, Dr. T. Oka for the software for the digital signal

processing, and Dr. M. Yamaguchi of the Jikei Medical School for help in part of the experiment. The x-ray experiments were performed under approval of the SPring-8 Proposal Review Committee (2001A0402, 2001B0089, 2002B0137, 2003A0165, 2003B0179).

REFERENCES

1. Claflin, D. R., D. L. Morgan, and F. J. Julian. 1990. Earliest mechanical evidence of cross-bridge activity after stimulation of single skeletal muscle fibers. *Biophys. J.* 57:425–432.
2. Proske, U., and D. L. Morgan. 1999. Do cross-bridges contribute to the tension during stretch of passive muscle? *J. Muscle Res. Cell Motil.* 20: 433–442.
3. Sandow, A. 1944. Studies on the latent period of muscular contraction. Method. General properties of latency relaxation. *J. Cell. Comp. Physiol.* 24:221–256.
4. Abbott, B. C., and J. M. Ritchie. 1951. Early tension relaxation during a muscle twitch. *J. Physiol.* 113:330–335.
5. Close, R. I. 1981. Activation delays in frog twitch muscle fibres. *J. Physiol.* 313:81–100.
6. Haugen, P., and O. Sten-Knüdsen. 1976. Sarcomere lengthening and tension drop in the latent period of isolated frog skeletal muscle fibers. *J. Gen. Physiol.* 68:247–265.
7. Rauh, F. 1920. Die Latenzzeit des Muskelelementes. *Z. Biol.* 76:25–48.
8. Close, R. I., and J. I. Lännergren. 1984. Arsenazo III calcium transients and latency relaxation in frog skeletal muscle fibres at different sarcomere lengths. *J. Physiol.* 355:323–344.
9. Baylor, S. M., and S. Hollingworth. 2000. Measurement and interpretation of cytoplasmic [Ca^{2+}] signals from calcium-indicator dyes. *News Physiol. Sci.* 15:19–26.
10. Hill, D. K. 1968. Tension due to interaction between the sliding filaments in resting striated muscle. The effect of stimulation. *J. Physiol.* 199:637–684.
11. Wang, K., R. McCarter, J. Wright, J. Beverly, and R. Ramirez-Mitchell. 1991. Regulation of skeletal muscle stiffness and elasticity by titin isoforms: a test of the segmental extension model of resting tension. *Proc. Natl. Acad. Sci. USA.* 88:7101–7105.
12. Maruyama, K. 1997. Connectin/titin, giant elastic protein of muscle. *FASEB J.* 11:341–345.
13. Labeit, D., K. Watanabe, C. Witt, H. Fujita, Y. Wu, S. Lahmers, T. Funck, S. Labeit, and H. L. Granzier. 2003. Calcium-dependent molecular spring elements in the giant protein titin. *Proc. Natl. Acad. Sci. USA.* 100:13716–13721.
14. Tatsumi, R., K. Maeda, A. Hattori, and K. Takahashi. 2001. Calcium binding to an elastic portion of connectin/titin filaments. *J. Muscle Res. Cell Motil.* 22:149–162.
15. Yagi, N. 2003. An x-ray diffraction study on early structural changes in skeletal muscle contraction. *Biophys. J.* 84:1093–1102.
16. Inoue, K., T. Oka, T. Suzuki, N. Yagi, K. Takeshita, S. Goto, and T. Ishikawa. 2001. Present status of high flux beamline (BL40XU) at SPring-8. *Nucl Instrum Meth A.* 467–468:674–677.
17. Amemiya, Y., K. Ito, N. Yagi, Y. Asano, K. Wakabayashi, T. Ueki, and T. Endo. 1995. Large-aperture TV detector with a beryllium-windowed image intensifier for x-ray diffraction. *Rev. Sci. Instrum.* 66:2290–2294.
18. Yagi, N., K. Inoue, and T. Oka. 2004. CCD-based x-ray area detectors for time-resolved experiments. *J Synchrotron Rad.* 11:456–461.
19. Wakayama, J., T. Tamura, N. Yagi, and H. Iwamoto. 2004. Structural transients of contractile proteins upon sudden ATP liberation in skeletal muscle fibers. *Biophys. J.* 87:430–441.
20. Huxley, H. E., and W. Brown. 1967. The low-angle x-ray diagram of vertebrate striated muscle and its behavior during contraction and rigor. *J. Mol. Biol.* 30:383–434.
21. Craig, R., and G. W. Offer. 1976. Axial arrangement of crossbridges in thick filaments of vertebrate skeletal muscle. *J. Mol. Biol.* 102:325–332.
22. Malinchik, S. B., and V. V. Lednev. 1992. Interpretation of the x-ray diffraction pattern from relaxed skeletal muscle and modelling of the thick filament structure. *J. Muscle Res. Cell Motil.* 13:406–419.
23. Huxley, H. E., A. R. Faruqi, M. Kress, J. Bordas, and M. H. J. Koch. 1982. Time-resolved x-ray diffraction studies of the myosin layer-line reflections during muscle contraction. *J. Mol. Biol.* 158:637–684.
24. Gilai, A., and G. E. Kirsch. 1978. Latency-relaxation in single muscle fibres. *J. Physiol.* 282:197–205.
25. Huxley, A. F., and L. D. Peachey. 1961. The maximum length for contraction in vertebrate striated muscle. *J. Physiol.* 156:150–165.
26. Haselgrove, J. C. 1975. X-ray evidence for conformational changes in the myosin filaments of vertebrate striated muscle. *J. Mol. Biol.* 92:113–143.
27. Yagi, N., and I. Matsubara. 1980. Myosin heads do not move on activation in highly stretched vertebrate striated muscle. *Science.* 207:307–308.
28. Linari, M., G. Piazzesi, I. Dobbie, N. Koubassova, M. Reconditi, T. Narayanan, O. Diat, M. Irving, and V. Lombardi. 2000. Interference fine structure and sarcomere length dependence of the axial x-ray pattern from active single muscle fibers. *Proc. Natl. Acad. Sci. USA.* 97:7226–7231.
29. Yagi, N., and I. Matsubara. 1989. Structural changes in the thin filament during activation studied by x-ray diffraction of highly stretched skeletal muscle. *J. Mol. Biol.* 208:359–363.
30. Huxley, H. E., A. A. Stewart, H. Sosa, and T. C. Irving. 1994. X-ray diffraction measurements of the extensibility of actin and myosin filaments in contracting muscle. *Biophys. J.* 67:2411–2421.
31. Wakabayashi, K., Y. Sugimoto, H. Tanaka, Y. Ueno, Y. Takezawa, and Y. Amemiya. 1994. X-ray diffraction evidence for the extensibility of actin and myosin filaments during muscle contraction. *Biophys. J.* 67:2422–2435.
32. Bagshaw, C. R., and G. H. Reed. 1977. The significance of the slow dissociation of divalent metal ions from myosin ''regulatory'' light chains. *FEBS Lett.* 81:386–390.
33. Linari, M., I. Dobbie, M. Reconditi, N. Koubassova, M. Irving, G. Piazzesi, and V. Lombardi. 1998. The stiffness of skeletal muscle in isometric contraction and rigor: the fraction of myosin heads bound to actin. *Biophys. J.* 74:2459–2473.
34. Huxley, H. E., R. M. Simmons, A. R. Faruqi, M. Kress, J. Bordas, and M. H. J. Koch. 1983. Changes in the x-ray reflections from contracting muscle during rapid mechanical transients and their structural implications. *J. Mol. Biol.* 169:469–506.
35. Yagi, N., H. Iwamoto, J. Wakayama, and K. Inoue. 2005. Structural changes of actin-bound myosin heads after a quick length change in frog skeletal muscle. *Biophys. J.* 89:1150–1164.
36. Piazzesi, G., M. Reconditi, I. Dobbie, M. Linari, P. Boesecke, O. Diat, M. Irving, and V. Lombardi. 1999. Changes in conformation of myosin heads during the development of isometric contraction and rapid shortening in single frog muscle fibres. *J. Physiol.* 514:305–312.
37. Yagi, N., E. J. O'Brien, and I. Matsubara. 1981. Changes of thick filament structure during contraction of frog striated muscle. *Biophys. J.* 33:121–138.